Implementation of closed-loop field-oriented control for PMSM on rehabilitation robot using BTS 7960

Vita Ayu Nathalia, Dimas Adiputra, Rifki Dwi Putranto
Department of Electrical Engineering, Faculty of Electrical Engineering, Telkom University, Surabaya, Indonesia

Article Info	ABSTRACT
	The efficiency of control systems in permanent magnet synchronous motors (PMSM) is crucial, especially for applications in physiotherapy robots. Previous studies have demonstrated that an open-loop field-oriented control (FOC) driver using BTS7960 outperforms the commonly used electronic speed controller (ESC). This research addresses the challenge of further improving efficiency by employing a closed-loop FOC driver with the BTS7960. The research methodology involves two main stages. First, a PSIM software simulation of a closed-loop FOC using a proportional integral (PI) controller is conducted. The aim is to determine the P and I parameters that result in the smallest settling time, steady-state error, and overshoot in controlling the PMSM motor's rotation per minute (RPM). The second stage involves hardware implementation with the BTS7960, where the PMSM motor RPM is compared under various loads ranging from 10-gram to 60-gram. RPM results from both open-loop and closed-loop configurations are compared. The results show that the closed-loop FOC driver has improved system transient response compared to the previous open-loop FOC driver, notably reducing the settling time from 2.24 seconds to 1.45 seconds for a 60-gram load. Therefore, this research concludes that a closed-loop configuration with well-tuned PI parameters can deliver better performance compared to open-loop methods, as clearly demonstrated.

Corresponding Author:

Dimas Adiputra
Department of Electrical Engineering, Faculty of Electrical Engineering, Telkom University
Ketintang Street 156, Gayungan, Surabaya 60231, Indonesia
Email: dimasze@telkomuniversity.ac.id

1. INTRODUCTION

To achieve a more sustainable and inclusive global future, the Sustainable Development Goals (SDGs) initiated by the United Nations (UN) play a crucial role in guiding countries worldwide toward better outcomes [1]. Among the 17 goals outlined in the SDGs, ensuring equitable health and well-being for all, represented by SDG 3, holds a very important position. SDG 3 focuses on providing fair and universal access to quality healthcare services and promoting well-being for everyone, regardless of their socioeconomic background. Achieving this goal requires not only overall improvements in health systems but also innovations in treatment and rehabilitation, especially for significant diseases like stroke [2], [3].

Stroke is one of the most serious and debilitating diseases globally. In general, a stroke occurs when blood flow to the brain is disrupted, which can cause significant damage to brain tissue and affect various bodily functions. This damage often results in long-term disability, with paralysis being one of the most common complications [4], [5]. The impact of stroke extends beyond the individual, creating a substantial social and economic burden on families and communities due to the long-term care and rehabilitation required. Given the significant challenges posed by stroke, improving the quality of rehabilitation services is crucial [6].

In this context, technical developments like the creation of physiotherapy robots offer promising alternatives for enhancing rehabilitation effectiveness and efficiency. Physiotherapy robots, particularly those based on ankle-foot orthoses (AFO), are designed to assist patients with motor impairments due to stroke in their rehabilitation, focusing on recovering walking ability and balance. AFOs are medical devices specifically designed to support the foot, ankle, and lower limbs, helping patients with foot drop, ankle bone abnormalities, and balance difficulties [7], [8].

In designing ankle-foot orthoses (AFO), one key component is the permanent magnet synchronous motor (PMSM), used as an actuator in the robot due to its advantages in torque density and back drivability [9]. To fully utilize these advantages, a proper control system is needed to manage and regulate PMSM operations, including speed, torque, and motor position, according to rehabilitation needs. One commonly used control method for managing PMSM in AFOs is field-oriented control (FOC). FOC is a control approach for AC motors similar to DC motor control methods, where the principle is to separate the control of current in the motor's excitation and load sections, allowing independent control of flux and torque. FOC provides fast torque responses for optimal performance and precision in various applications [10], [11].

Previous research compared the performance of BLDC motors controlled by field-oriented control (FOC) and electronic speed control (ESC) through testing. Tests using FOC with BTS 7960 and ESC showed that FOC with BTS 7960 achieved higher speeds and greater torque (0.8%) compared to ESC, which had lower torque. Based on these results, FOC with BTS 7960 is concluded to be a more optimal choice for rehabilitation robots. However, FOC controllers have limitations, such as not achieving maximum torque, which requires a complex electronic configuration for optimal performance [12].

Building on previous research, this study will advance by implementing closed-loop field-oriented control (FOC) with BTS 7960. This system can provide feedback on output voltage when using PMSM motors to achieve better results. A closed-loop system optimizes feedback from sensors to dynamically measure and correct motor performance based on actual conditions. By using sensors such as encoders, closed-loop control can continuously monitor parameters such as speed, torque, and motor position, and respond quickly to changes in load or operational conditions. This ensures that the motor operates according to the desired setpoint, enhancing performance, precision, and stability [13]. In contrast, an open-loop system only responds to predetermined commands without adjusting for changes in load or working conditions, making it less responsive to unexpected changes in the operational environment. By integrating closed-loop control, this study makes a significant contribution to new knowledge by introducing a more adaptive and precise motor control technology, offering new insights into more effective control strategies in the context of PMSM motor applications [14], [15].

2. METHOD
2.1. Research flow

The research flow related to the implementation of closed-loop FOC controllers for PMSM motors on rehabilitation robots involves several steps as shown in Figure 1. The initial research began with designing a closed-loop FOC system using software. The next step is determining parameters to produce a fast output response so that the hardware design of the closed-loop FOC control system using BTS 7960 could be continued. After that, it was finished when the test result shows that the controller can move the motor [16], [17].

2.2. Open loop FOC for RPM control

Open-loop field-oriented control (FOC) is a motor control method designed to regulate PMSM in a relatively simple manner, but with limitations in responding to dynamic changes in operating conditions. In an open-loop FOC system, motor control is based on predefined settings without real-time feedback [18], [19]. In open-loop FOC, the commutation voltage for the motor is set using fixed frequency and phase relationships. These settings are based on a constant input signal, which includes the desired speed and torque. The commutation voltage is then directly applied to the motor to achieve the target rotational speed [20], [21]. This system operates under the assumption that the motor's operating conditions, such as load and performance, remain stable and do not change significantly. The main advantage of open-loop FOC is its simplicity in design and implementation [22]. Since it does not require feedback sensors, the system reduces the complexity of the hardware and software needed for motor control. Additionally, open-loop FOC can be more cost-effective because it does not require additional components for real-time measurement and adjustment [23]-[25].

However, there are several significant limitations to this method. Without real-time feedback, an open-loop FOC system cannot adjust to sudden changes in motor performance or load. For example, if there is a variation in load or external disturbances, the open-loop FOC cannot automatically correct the commutation settings, which can result in less accurate speed control and reduced motor efficiency. This can lead to fluctuations in motor performance and an inability to achieve the desired torque and speed with high precision [26], [27]. Figure 2 presents the block diagram used in the open-loop FOC method.

2.3. Closed-loop FOC for RPM control

Field orientation control (FOC) is an approach to control AC motors that is similar to the control method for DC motors, where the principle is to separate current control in the amplifier section and the load section of the motor. As shown in Figure 3, the block diagram of the closed-loop field-oriented control (FOC) method compares the reference speed (RPM) with the actual speed (RPM) of the motor. The reference speed (RPM) is compared with the actual speed (RPM) of the motor [28]. The difference between these two speeds, or rather the RPM error, is then fed into the proportional integral (PI) controller to produce a control signal (W). The control signal (W) produced by the PI controller is then transformed to produce a commutation voltage (Va, Vb, Vc) that corresponds to the motor phases. In this transformation, the commutation voltage for each motor phase is calculated based on time (t) and control signal frequency (W). The Vpeak is the maximum voltage given to the motor. For instance, if the motor is supplied by 5 V, then the Vpeak is 5. The equations used to calculate commutation voltage are (1)-(3).

$$Va = Vpeak/2 + Vpeak/2 * sin(W * t) \tag{1}$$

$$Vb = Vpeak/2 + Vpeak/2 * sin(W * t + 2\pi/3) \tag{2}$$

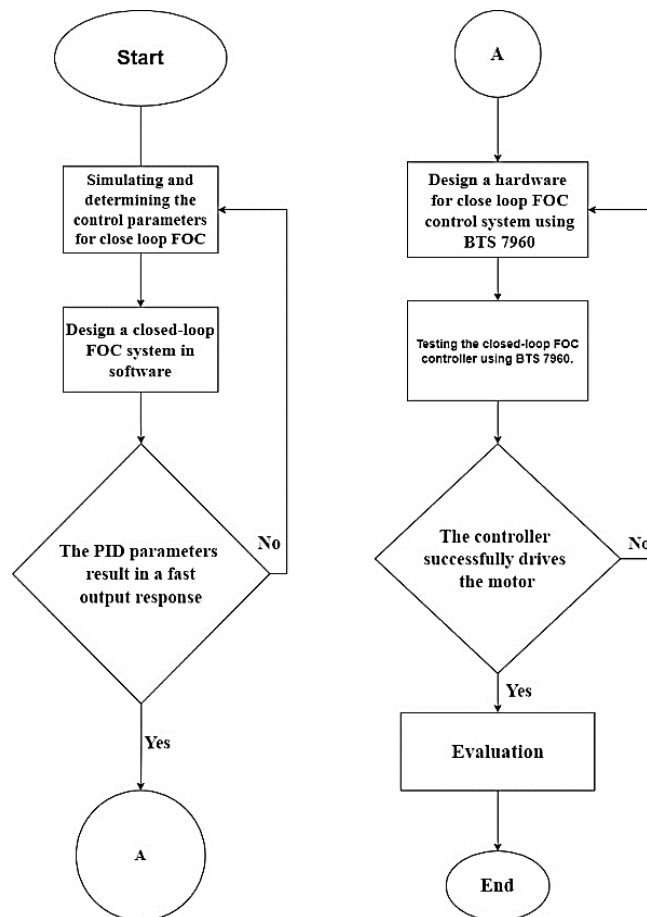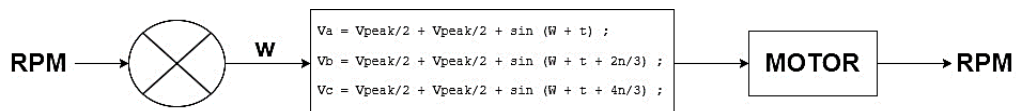$$Vc = Vpeak/2 + Vpeak/2 * sin(W * t + 4\pi/3) \tag{3}$$

Figure 1. Research flow

Figure 2. Open-loop FOC method block diagram

For simulation, the Vpeak is filled with the desired maximum voltage. As for the implementation on Arduino, the Vpeak is filled with the maximum pulse width modulation (PWM) duty cycle, which is 255 to represent 100% duty cycle. This is due to the maximum voltage correlating with 100% duty cycle [12]. The encoder sensor provides real-time feedback, allowing the system to dynamically adjust the control signal, handle load variations and external disturbances, and ensure more accurate and responsive motor performance. The integration of the encoder sensor in the closed-loop FOC system allows for more precise and efficient adjustments, resulting in optimal motor control with reduced steady-state error and overshoot [29], [30].

2.4. Simulation on PSIM software

In this study, a closed-loop system is simulated using power system simulation software (PSIM), which is software for designing, analyzing, and testing electrical and power electronic systems [31]. The design of the closed-loop field-oriented control system is illustrated in Figure 4 and is divided into four parts. The first part (I) shows the control signal and signal converter (c/p) that transforms the current signals (Ia, Ib, Ic) from control signals to power signals. The second part (II) features a PMSM block and a rotary encoder to measure the motor's RPM. The third part (III) is the FOC controller represented by a C-Block. The C-Block receives the current RPM and generates the current signal for the first part. It also produces the control frequency (W) for measurement purposes. Finally, the fourth part (IV) displays the clock to run the simulation.

The PMSM motor block enables virtual simulation of the motor's characteristics and behavior. Motor specifications can be adjusted, allowing for performance analysis in a virtual environment and more effective control optimization [32]. In this study, the BM 4108 380 KV motor is modeled using the PMSM block. Table 1 shows the parameters of the BM 4108 380 KV motor [33]. After setting the motor parameters, the next step is to conduct open-loop simulation testing with load variations from 10 to 60 grams. Subsequently, experiments are conducted on parameters such as P and I to achieve the most optimal transient response. The selection of P and I parameters is done through an initial trial approach. For example, starting with initial values of $Kp = 2$ and $Ki = 10$. After analyzing the simulation results with these values, it was found that the system's performance did not meet the desired target. Therefore, these parameter values are gradually increased in certain increments until an optimal parameter combination is found that provides the best system response. This process involves repeatedly adjusting Kp and Ki until parameters are found that meet the criteria for system performance, such as minimal overshoot and the fastest settling time. These optimal values are then retested with load variations from 10 to 60 grams to ensure consistent performance under various conditions.
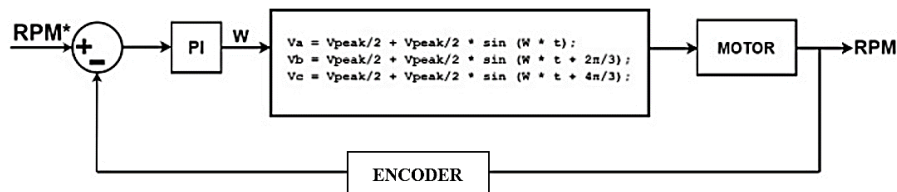
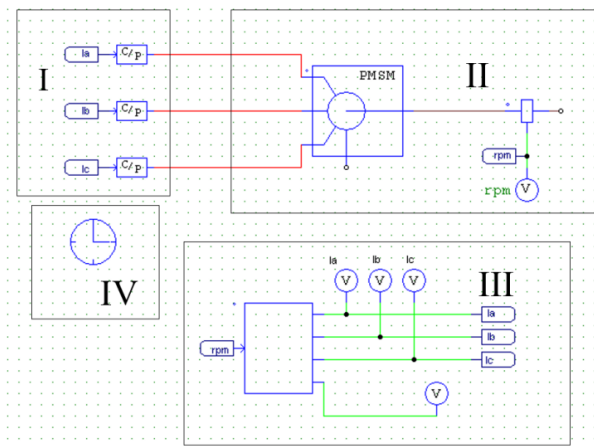Figure 3. Closed-loop field-oriented control (FOC) method block diagram

Figure 4. Designing a closed-loop field-oriented control simulation on PSIM software

2.5. Implementation using BTS 7960

The closed-loop FOC control system using BTS 7960 involves a PMSM motor as an actuator and BTS 7960 as the motor driver, as depicted in Figure 5(a) displays the schematic of the closed-loop field-oriented control (FOC) system using BTS 7960 motor drivers. This schematic provides a visual representation of how the various components in the system are connected and work together and Figure 5(b) in the implementation, the hardware design includes Arduino Uno as the microcontroller, three BTS 7960 motor drivers, a power supply, PMSM motor model BM 4108 380 KV as the system output, and a hall sensor (AS5600 Magnetic Encoder) as a feedback sensor.

Table 1. Modeling a PMSM in PSIM software

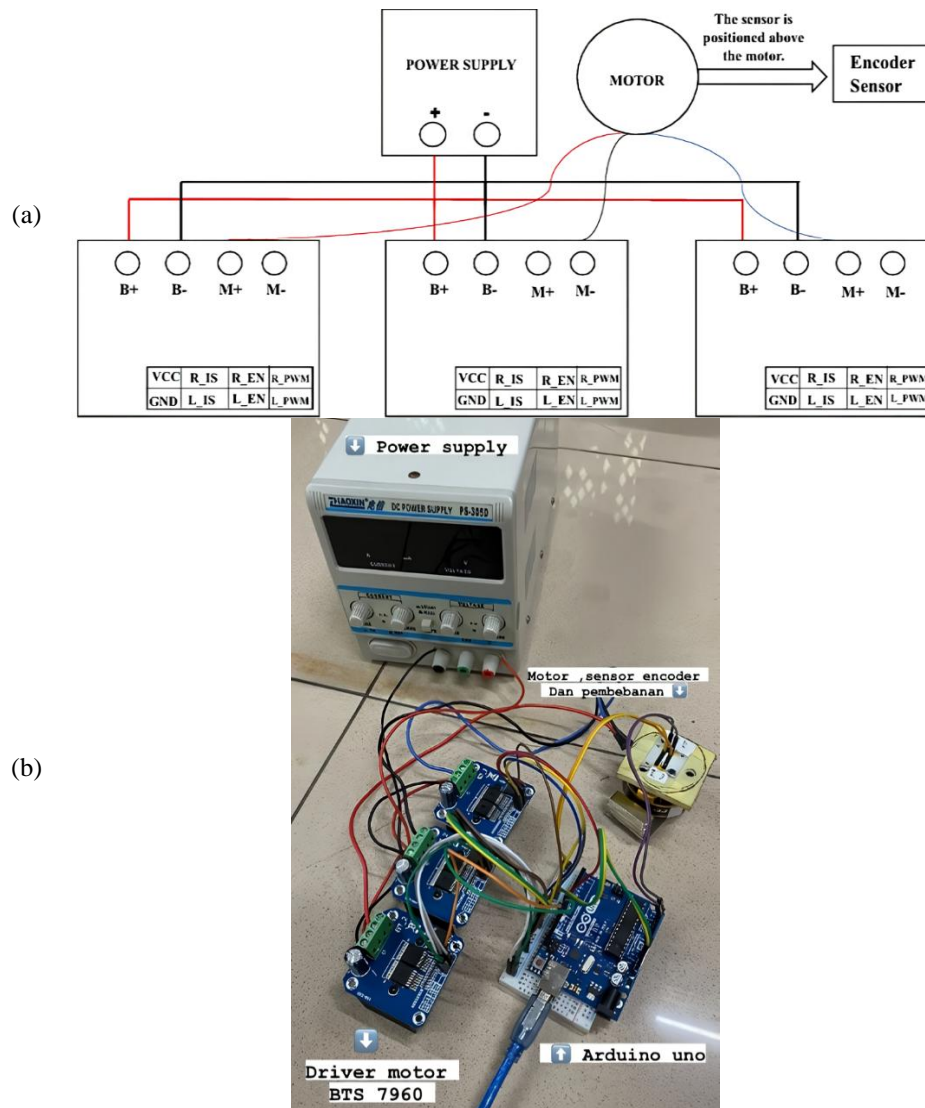| Parameter name	Value
Rs (stator resistance)	0.193 Ω
Ld (d-axis ind.)	0.1303 mH
Lq (q-axis ind.)	0.1814 mH
Vpk/krpm	0.004824
No. of poles P	4
Moment of inertia	0.000065 kg·m²
Mech. time constant	10 s
Torque flag	1
Master/slave flag	1

Figure 5. Closed-loop field-oriented control system using BTS 7960: (a) schematic and (b) implementation

The power supply provides voltage to the motor, which is controlled by Arduino control signals based on the FOC algorithm [34]. These signals are sent through three BTS 7960 motor drivers, with each motor driver pin playing a specific role. Here, if the power signal comes from M+, then the control pin is the R_PWM pin. If the power signal comes from M-, then the control pin is the L_PWM pin. On the Arduino, the corresponding pin to generate a PWM signal is pin 9, 10, and 11, which produce a 490 Hz PWM signal. The PMSM motor then receives the controlled voltages, processes them to generate position and RPM feedback through the Hall sensor. In PMSM motor control, the signal feedback on each channel (A, B, C) is commonly collected using the Hall sensor for efficient control [12]. But, in this study, the Hall sensor collects the motor RPM instead.

Similar testing scenarios as in the simulation are taken. First, open loop conditions are tested for various loads from 10 to 60 grams, where constant W is given to the controller. Then, closed loop conditions are tested, where the optimal PI controller obtained from the simulation is used. Transient response, such as overshoot and settling time, is observed.

3. RESULTS AND DISCUSSION

This section presents two main results: simulation and implementation on both open-loop and closed-loop systems. The simulation results offer theoretical predictions of system behavior, while the implementation results provide empirical data that validate the system's performance under various conditions.

3.1. Simulation
3.1.1. Open-loop

The researcher discusses the simulation results of field-oriented control (FOC) using PSIM software, including both open-loop and closed-loop conditions, with tests conducted across various loads to understand the control system's response comprehensively. In the open-loop condition, various load variations were applied to the system with key parameters [35], [36]. Table 1 presents the results of the tested load variations, ranging from 10 to 60 grams. The analysis focuses on four parameters: RPM, steady-state error, overshoot, and set point. These parameters provide significant insights into the system's response to load variations.

The data in Table 2 illustrates the system's response variations to changes in motor load in an open-loop condition, where an increase in load influences torque despite the motor RPM remaining at 7.3. The system's stabilization time also shows an increase with the load, indicating the complexity of the system's response to changing conditions. A consistent steady-state error of 75.67% indicates the system's inability to reach the 30 RPM set point, reflecting a limitation that needs to be addressed. Although the overshoot decreases with an increase in load, its level remains high and can impact the system's performance in reaching the set point. This analysis concludes that system improvement is needed through the implementation of a closed-loop control system, which is expected to minimize steady-state error, reduce overshoot, and enhance the system's response to changing conditions. Thus, the use of a closed-loop is anticipated to improve system accuracy and stability, enabling the achievement of set point values with greater precision. Figure 6(a) shows the simulation results graph of speed with a 60-gram load in the open loop condition, while Figure 6(b) presents the simulation results graph of torque with a 60-gram load in the open loop condition.

Table 2. The simulation results with various load variations in the open-loop condition

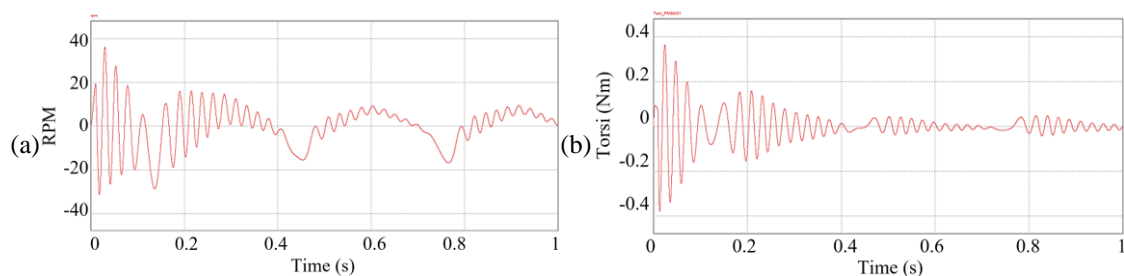| Load (gram)	RPM	Torsi (Nm)	Settling time (s)	Steady state error (%)	Overshoot (RPM)	Set point (RPM)
10	7.3	0.00329	0.29	75.67%	191	30
20	7.3	0.0066	0.6	75.67%	110	30
30	7.3	0.0088	0.65	75.67%	57	30
40	7.3	0.00923	0.71	75.67%	41	30
50	7.3	0.0098	0.85	75.67%	37	30
60	7.3	0.0135	0.98	75.67%	37	30

Figure 6. The simulation results for a 60-gram load in an open-loop condition: (a) RPM and (b) torque

3.1.2. Closed-loop

In the closed-loop condition, control parameters KP (proportional gain) and KI (integral gain) significantly affect performance and system response. Table 3 presents the results of tests involving variations in KP and KI values, considering parameters such as settling time, steady-state error, and overshoot. Table 3, considering three control system parameters, namely settling time, steady-state error, and overshoot, during the testing of load variations with different combinations of KP and KI values, the results indicate that the first configuration with KP at 6 and KI at 100 provides fast stabilization time at 0.27 seconds and an overshoot of 35 RPM, although with a slightly negative torque of -0.0217, indicating a good response to system changes. The second configuration with KP at 4 and KI at 100 shows slower stabilization time but a more stable response with a small torque of 0.0028. The third test with KP at 10 and KI at 60 demonstrates fast stabilization time at 0.4 seconds and a low overshoot of 17, creating a balance between stabilization time and overshoot, although with a high torque of 0.316. The fourth test with KP at 10 and KI at 100 has a fast stabilization time at 0.35 seconds but a high overshoot of 60 RPM and a high torque of 0.03, affecting system performance. The fifth test with KP at 10 and KI at 50 shows fast stabilization time at 0.259 seconds but a very high overshoot of 182 RPM with a torque of 0.288. The last test with KP at 10 and KI at 200 has a fast stabilization time at 0.27 seconds, a low overshoot of 40, and a lower torque of 0.0281.

Based on the analysis, it can be concluded that the values of KP and KI significantly impact the control system. The interaction between the two creates a balance between fast response and stability. The optimal combination appears to be KP at 6 and KI at 100, demonstrating optimal performance with fast settling time, low steady-state error, and minimal overshoot. Therefore, in this testing condition, optimization with KP at 6 and KI at 100 is identified as the most effective parameter choice. After previously discussing the characteristics of the control system with proportional (KP) and integral (KI) parameters set at values of 60 and 100, the next step is to apply these parameters in a variation test.

Table 4 displays the simulation results of loading variations with KP at 60 and KI at 100 in the closed-loop condition, focusing on three control system parameters: settling time, steady-state error, and overshoot. For a 10-gram load variation, a high positive torque of 0.383 reflects a very good system response with a relatively fast settling time at 0.39 seconds and a steady-state error of 0%. However, the high overshoot of 211 RPM indicates oscillations after reaching the set point, requiring further adjustments in the control system. In the case of a 20-gram load variation, the lower positive torque of 0.0495 indicates a slightly weaker response, with a slightly longer settling time at 0.78 seconds and a steady-state error of 0%, but oscillations are still present. As the load increases to 30 grams, the lower positive torque of 0.00349 indicates a lower response, with a longer settling time at 1.17 seconds and a lower overshoot of 27, showing an improvement in system stability. For a 40-gram load variation, the increased positive torque of 0.211, with a lower overshoot of 22.9 reflects a stronger response and increased stability.

Table 3. Simulation results from testing several variations of KP and KI parameters

KP	Ki	RPM	Torsi (Nm)	Settling time (s)	Steady state error (%)	Overshoot (RPM)	w
6	100	20	0.176	0.25	0%	37	36
4	100	20	0.0194	0.4	0%	31.5	33
10	60	20	0.316	0.4	0%	17	13
10	100	20	0.03	0.35	0%	60	51
10	50	20	0.288	0.259	0%	182	13
10	200	20	0.0281	0.27	0%	40	17

Table 4. The loading variations in the closed-loop system with optimal parameters

KP	Ki	Load (gram)	RPM	Torsi (Nm)	Settling time (s)	Steady state error (%)	Overshoot (RPM)
6	100	10	20	0.383	0.39	0%	211
6	100	20	20	0.0495	0.78	0%	38
6	100	30	20	0.00349	1.17	0%	27
6	100	40	20	0.211	1.28	0%	22.9
6	100	50	20	0.154	1.53	0%	21
6	100	60	20	-0.205	1.75	0%	21

However, the settling time continues to increase to 1.28 seconds, indicating increased system complexity with a heavier load. When the load is increased to 50 grams, the lower positive torque of 0.154 and the continued increase in settling time to 1.53 seconds indicate a slower response, although the overshoot remains relatively low at 21. For a 60-gram load variation, a negative torque of -0.205 and a change in polarity require special attention. Despite a steady-state error of 0%, the settling time continues to increase to 1.75 seconds, indicating a progressively slower system response, and the change in polarity requires further analysis. Figures 7(a) and 7(b) visually depict changes in the system response to a 60-gram load variation,

showing a significant impact on motor torque and RPM. Load changes result in changes in the required torque to maintain system stability, and the decrease in torque values at a 60-gram load indicates that the system has reached its capacity limit to handle higher loads.

From the simulation results, it can be concluded that the closed-loop system is significantly superior to the open-loop system in terms of accuracy and stability. Although the closed-loop system has a slightly longer settling time, its advantage is evident in its ability to reach the desired set point and handle disturbances and load variations. In contrast, the open-loop system exhibits higher overshoot, greater oscillations, and significant steady-state errors, indicating its limitations in effective control. Therefore, the closed-loop system, especially with optimized KP and KI parameters, delivers better performance, demonstrating a more stable and accurate response to changes in conditions and loads.
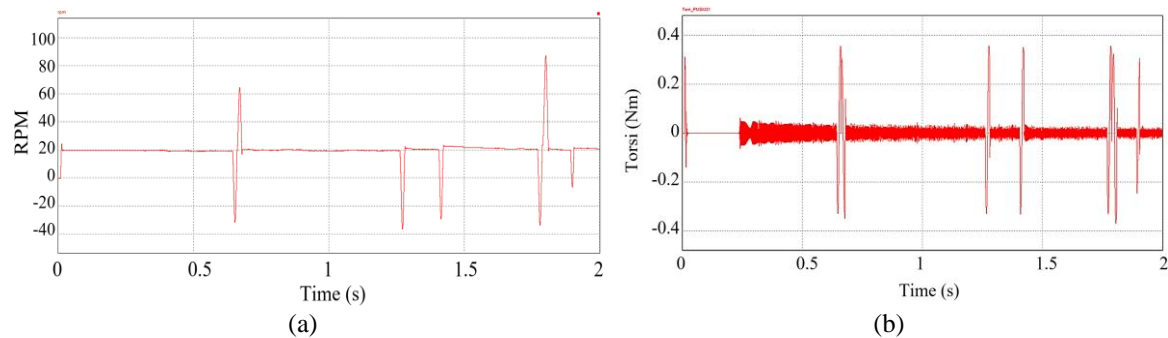
Figure 7. The simulation results for a 60-gram load in a closed-loop condition: (a) RPM and (b) torque

3.2. Implementation
3.2.1. Open loop

In the implementation of an open-loop system utilizing the BTS7960 motor driver, various load variations were systematically introduced to assess the system's performance across key parameters. The load variations, which ranged from 10 to 60 grams, were carefully tested to observe their impact on the system's behavior. The results of these tests, highlighting the system's response under different loading conditions, are comprehensively presented in Table 5.

In the implementation under open-loop conditions, with a 10-gram load, the system exhibits a very low settling time, indicating a rapid response to light loads. However, as the load increases, such as at 20-grams, 30-grams, 40-grams, 50-grams, and 60-grams, the settling time tends to increase. This suggests that the system becomes less responsive and requires better adjustments to handle heavier load variations. To optimize system performance, especially under heavier loads, the implementation of proportional and integral (PI) control can be an effective solution. This control can help reduce steady-state errors in the system, enhance stability, and expedite settling time. By designing appropriate PI control parameters, the system can efficiently respond to load changes, optimize response, and maintain stability under various operational conditions. Figure 8 illustrates the graph of the 60-gram load implementation under open-loop conditions.

3.2.2. Closed-loop

During the closed-loop implementation of the field-oriented control (FOC) system, load variations ranging from 10 to 60 grams were introduced to examine key parameters. The analysis focused on RPM and settling time, offering insights into the system's response to these variations. The results of these tests are detailed in Table 6.

Table 5. The results of the control system implementation with various load variations in an open-loop condition

Load (gram)	RPM	Settling time (s)	Overshoot (RPM)
10	20	0.52	23
20	20	1.17	20
30	20	1.27	38
40	20	1.39	37
50	20	1.47	33
60	20	2.24	21

Application of PI control in a closed-loop control system with load variations, there is a noticeable improvement in response for a 10-gram load, with a reduced settling time from 0.52 seconds to 0.36 seconds and an overshoot of 21, indicating system optimization for more efficient response to light loads. For a 20-gram load, PI control continues to play a role in maintaining system stability with an acceptable increase in settling time to 0.52 seconds and an overshoot of 20. With a 30-gram load, PI control enhances the adaptability of the system with a significant decrease in settling time from 1.27 seconds to 0.78 seconds and an overshoot of 21. Although there is a moderate increase in settling time from 1.39 seconds to 0.84 seconds for a 40-gram load, PI control still maintains an efficient system response. For 50-gram and 60-gram loads, PI control provides significant improvement, albeit with an increase in settling time, with an overshoot of 20 for 50 grams and 21 for 60 grams. From this evaluation, it can be concluded that PI control plays a crucial role in optimizing the system's response to load variations, allowing for increased response speed, reduced overshoot, and overall system stability. Figure 9 illustrates the graph of the 60-gram load implementation in a closed-loop condition.

The comparison between open-loop and closed-loop control systems in implementation demonstrates the superiority of the closed-loop configuration in terms of stability and responsiveness. The closed-loop system has a lower average settling time (0.825 seconds) and smaller overshoot (21.17%) compared to the open-loop system, which has an average settling time of 1.35 seconds and an overshoot of 28.67%. This indicates that the closed-loop system provides better control, faster stabilization, and more accurate responses to input changes. Although the open-loop system is simpler, the closed-loop system offers greater flexibility and adaptability [37], [38], making it more suitable for applications requiring high stability and precision. However, challenges such as motor vibration and insufficient current data in the FOC implementation on PMSM motors can affect the quality of movement and system stability, indicating the need for further refinement [39], [40].
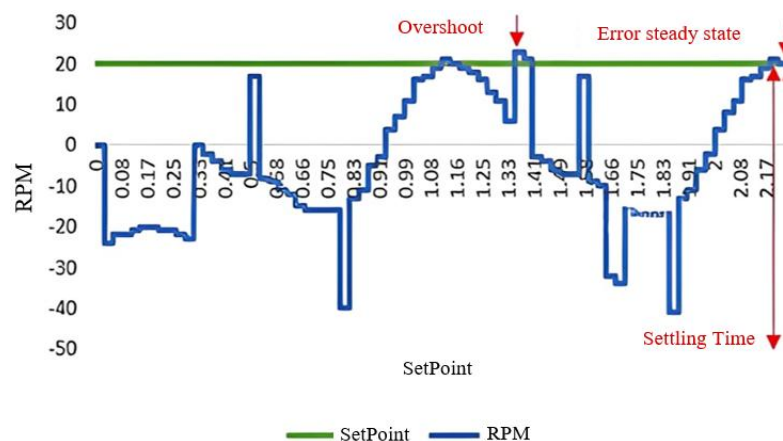

Figure 8. Graph of the implementation of a 60-gram load under open loop conditions
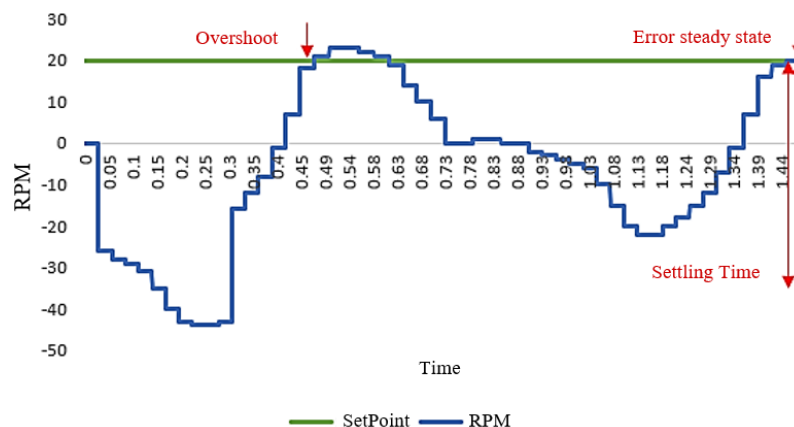

Figure 9. Graph of the implementation of a 60-gram load under closed-loop condition

Table 6. The results of the control system implementation with various load variations
in a closed-loop condition

Load (gram)	RPM	Settling time	Overshoot (RPM)
10	20	0.36	21
20	20	0.52	20
30	20	0.78	21
40	20	0.84	22
50	20	1.41	20
60	20	1.45	21

4. CONCLUSION

This research successfully simulated and determined the closed-loop field-oriented control (FOC) on permanent magnet synchronous motor (PMSM) within the context of rehabilitation robots. Simulation results indicate that the implementation of closed-loop FOC, particularly with PI control and adjustment of KP and KI values, significantly enhances system response compared to the open-loop condition. The KP and KI values used were 60 and 100, demonstrating that closed-loop performs better than open-loop, especially in response to load variations from 10 to 60 grams. However, the implementation of closed-loop FOC using BTS 7960 reveals challenges such as less smooth vibrations at low speeds, caused by magnet phenomena (cogging), and unstable motor movements. Insufficient current data also affects the stability and smoothness of the motor's motion, despite efforts to improve the data.

AUTHOR CONTRIBUTIONS STATEMENT

This journal uses the Contributor Roles Taxonomy (CRediT) to recognize individual author contributions, reduce authorship disputes, and facilitate collaboration.

Name of Author	C	M	So	Va	Fo	I	R	D	O	E	Vi	Su	P	Fu
Vita Ayu Nathalia			✓	✓	✓	✓		✓	✓		✓			
Dimas Adiputra	✓	✓	✓		✓		✓			✓			✓	✓
Rifki Dwi Putranto				✓	✓					✓		✓		

C : **C**onceptualization
M : **M**ethodology
So : **So**ftware
Va : **Va**lidation
Fo : **Fo**rmal analysis

I : **I**nvestigation
R : **R**esources
D : **D**ata Curation
O : Writing - **O**riginal Draft
E : Writing - Review & **E**diting

Vi : **Vi**sualization
Su : **Su**pervision
P : **P**roject administration
Fu : **Fu**nding acquisition

CONFLICT OF INTEREST STATEMENT

The authors declare that there is no conflict of interest regarding the publication of this paper. All contributions were made in the interest of academic and scientific advancement without any commercial or financial relationships that could be construed as a potential conflict of interest.

DATA AVAILABILITY

The data supporting the findings of this study are available from the corresponding author, [DA], upon reasonable request. While rough or summarized data are presented within the paper, access to the complete and detailed dataset requires prior approval and may be granted for research and verification purposes.

REFERENCES

[1]   A. Kara, H. Zhou, and Y. Zhou, "Achieving the United Nations' sustainable development goals through financial inclusion: A systematic literature review of access to finance across the globe," *International Review of Financial Analysis*, vol. 77, p. 101833, Oct. 2021, doi: 10.1016/j.irfa.2021.101833.

[2]   L. D. Morris, K. A. Grimmer, A. Twizeyemariya, M. Coetzee, D. C. Leibbrandt, and Q. A. Louw, "Health system challenges affecting rehabilitation services in South Africa," *Disability and Rehabilitation*, vol. 43, no. 6, pp. 877–883, Mar. 2021, doi: 10.1080/09638288.2019.1641851.

[3]   T. Platz, *Clinical pathways in stroke rehabilitation*. Cham: Springer International Publishing, 2021. doi: 10.1007/978-3-030-58505-1.

[4]   B. Neurology, "Retracted: early stroke prediction methods for prevention of strokes," *Behavioural Neurology*, vol. 2023, no. 1, Dec. 2023, doi: 10.1155/2023/9784791.

[5]   B. H. Buck, N. Akhtar, A. Alrohimi, K. Khan, and A. Shuaib, "Stroke mimics: incidence, aetiology, clinical features and treatment," *Annals of Medicine*, vol. 53, no. 1, pp. 420–436, Jan. 2021, doi: 10.1080/07853890.2021.1890205.

[6]   C. Boehme, T. Toell, W. Lang, M. Knoflach, and S. Kiechl, "Longer term patient management following stroke: A systematic review," *International Journal of Stroke*, vol. 16, no. 8, pp. 917–926, Oct. 2021, doi: 10.1177/17474930211016963.

[7]   F. Alnajjar, R. Zaier, S. Khalid, and M. Gochoo, "Trends and technologies in rehabilitation of foot drop: a systematic review," *Expert Review of Medical Devices*, vol. 18, no. 1, pp. 31–46, Jan. 2021, doi: 10.1080/17434440.2021.1857729.

[8]   C. E. Ribeiro, "Design of a wearable active ankle-foot orthosis for both sides," Universidade do Minho, 201AD.

[9]   H. Zhu, "Design of a highly backdrivable, powered lower-limb orthosis for improved human interaction," The University of Texas at Dallas, 2020.

[10] A. Skuric, H. S. Bank, R. Unger, O. Williams, and D. González-Reyes, "SimpleFOC: A field oriented control (FOC) library for controlling brushless direct current (BLDC) and stepper motors," *Journal of Open Source Software*, vol. 7, no. 74, p. 4232, Jun. 2022, doi: 10.21105/joss.04232.

[11] A. Gholipour, M. Ghanbari, E. Alibeiki, and M. Jannati, "Sensorless FOC strategy for current sensor faults in three-phase induction motor drives," *Journal of Operation and Automation in Power Engineering*, vol. 11, no. 1, pp. 1–10, 2023, doi: 10.22098/JOAPE.2022.9274.1648.

[12] A. N. Halisyah, D. Adiputra, and A. Al Farouq, "Field oriented control driver development based on BTS7960 for physiotherapy robot implementation," *International Journal of Electrical and Computer Engineering (IJECE)*, vol. 14, no. 2, pp. 1486–1495, Apr. 2024, doi: 10.11591/ijece.v14i2.pp1486-1495.

[13] O. Saleem, M. Rizwan, and J. Iqbal, "Adaptive optimal control of under-actuated robotic systems using a self-regulating nonlinear weight-adjustment scheme: Formulation and experimental verification," *PLOS ONE*, vol. 18, no. 12, p. e0295153, Dec. 2023, doi: 10.1371/journal.pone.0295153.

[14] C. Camacho, H. Alvarez, J. Espin, and O. Camacho, "An internal model based—sliding mode control for open-loop unstable chemical processes with time delay," *ChemEngineering*, vol. 7, no. 3, p. 53, Jun. 2023, doi: 10.3390/chemengineering7030053.

[15] U. Montanaro, C. Chen, A. Rizzo, and A. Sorniotti, "Output-based enhanced closed-loop model reference adaptive control and its application to direct yaw moment control," *International Journal of Robust and Nonlinear Control*, vol. 34, no. 14, pp. 9471–9500, Sep. 2024, doi: 10.1002/rnc.7471.

[16] S. Tabet, A. Ghoggal, H. Razik, I. Amrani, and S. E. Zouzou, "Experimental and simulation investigation for rotor bar fault diagnosis in closed-loop induction motors drives," *Bulletin of Electrical Engineering and Informatics*, vol. 12, no. 4, pp. 2058–2068, Aug. 2023, doi: 10.11591/eei.v12i4.4833.

[17] M. Costin and C. Lazar, "Field-oriented predictive control structure for synchronous reluctance motors," *Machines*, vol. 11, no. 7, p. 682, Jun. 2023, doi: 10.3390/machines11070682.

[18] E. Frasca, "Design and testing of hardware in the loop test bench for permanent magnet synchronous motors controlled with field oriented control technique," Politecnico di Torino, 2022.

[19] P. Bernard, "Study of vector control strategy on interior permanent magnet synchronous motors," University West, 2023.

[20] Y. Guo, Y. Zhang, and X. Li, "Position correction control of permanent-magnet brushless motor based on commutation-interval current symmetry," *World Electric Vehicle Journal*, vol. 15, no. 5, p. 203, May 2024, doi: 10.3390/wevj15050203.

[21] O. A. Filina *et al.*, "Increasing the efficiency of diagnostics in the brush-commutator assembly of a direct current electric motor," *Energies*, vol. 17, no. 1, p. 17, Dec. 2023, doi: 10.3390/en17010017.

[22] A. Logren and L. Johansson, "Field-oriented control of PMSMs within CPU-constrained applications - firmware implementation of an FOC-based control strategy, focusing on robust CPU interrupt handling," 2024.

[23] D. Saputra, A. Ma'arif, H. Maghfiroh, P. Chotikunnan, and S. N. Rahmadhia, "Design and application of PLC-based speed control for DC motor using PID with identification system and MATLAB tuner," *International Journal of Robotics and Control Systems*, vol. 3, no. 2, pp. 233–244, Apr. 2023, doi: 10.31763/ijrcs.v3i2.775.

[24] A. Akhbari, M. Rahimi, and M. H. Khooban, "Direct current grid-based doubly-fed induction generator wind turbines: Real-time control and stability analysis," *IET Power Electronics*, vol. 15, no. 12, pp. 1158–1173, Sep. 2022, doi: 10.1049/pel2.12299.

[25] S. Mencou, M. Ben Yakhlef, and E. B. Tazi, "Advanced torque and speed control techniques for induction motor drives: A review," in *2022 2nd International Conference on Innovative Research in Applied Science, Engineering and Technology (IRASET)*, IEEE, Mar. 2022, pp. 1–9. doi: 10.1109/IRASET52964.2022.9738368.

[26] K. G. Tshamala, "Power hardware-in-the-loop emulation of a brushless DC motor," Concordia University, 2023.

[27] L. Wang, Y. Wu, X. Pan, and S. Hao, "Speed feedback observation algorithm based on parameter introduction and its application in asynchronous motor," *Proceedings of the Institution of Mechanical Engineers, Part I: Journal of Systems and Control Engineering*, vol. 237, no. 1, pp. 58–71, Jan. 2023, doi: 10.1177/09596518221119591.

[28] C. Wang, Y. Zhuang, J. Yang, Y. Liu, and J. Pan, "Characteristic analysis and control loop design of transmission torque and jerk for flexible joint servo systems," *IEEE Transactions on Power Electronics*, vol. 39, no. 7, pp. 8528–8539, Jul. 2024, doi: 10.1109/TPEL.2024.3382006.

[29] S. Cosso, "Study and analysis of controls for induction motor drives for high-power applications," University of Genoa, 2024.

[30] R. Wang *et al.*, "FI-NPI: Exploring optimal control in parallel platform systems," *Electronics*, vol. 13, no. 7, p. 1168, Mar. 2024, doi: 10.3390/electronics13071168.

[31] Y.-S. Lee, K.-M. Choo, W.-S. Jeong, C.-H. Lee, J. Yi, and C.-Y. Won, "A virtual impedance-based flying start considering transient characteristics for permanent magnet synchronous machine drive systems," *Energies*, vol. 16, no. 3, p. 1172, Jan. 2023, doi: 10.3390/en16031172.

[32] H. S. V. Pulakhandam, "System-level optimization methods for high-speed motor drives," North Carolina State University, 2023.

[33] C. R. Gade and R. S. Wahab, "Conceptual framework for modelling of an electric tractor and its performance analysis using a permanent magnet synchronous motor," *Sustainability*, vol. 15, no. 19, p. 14391, Sep. 2023, doi: 10.3390/su151914391.

[34] N. S. Rao *et al.*, "Monitoring and speed control of induction motor using Arduino," *International Journal of Progressive Research in Engineering Management and Science*, vol. 04, no. 03, pp. 274–279, Mar. 2024, doi: 10.58257/IJPREMS32900.

[35] V. K. Awaar, R. Simhadri, T. Jalla, M. Bagari, S. Aggarapu, and A. H. Abbas, "Parameter estimation and analysis of BLDC motor drive for electric vehicles application," *E3S Web of Conferences*, vol. 391, p. 01177, Jun. 2023, doi: 10.1051/e3sconf/202339101177.

[36] A. İ. Açıkgöz, "Comparison of speed control techniques in field oriented control of permanent magnet synchronous motor: Lyapunov approach," *Sigma Journal of Engineering and Natural Sciences – Sigma Mühendislik ve Fen Bilimleri Dergisi*, vol. 41, no. 6, pp. 1177–1196, 2023, doi: 10.14744/sigma.2023.00067.

[37] R. A. González, K. Classens, C. R. Rojas, J. S. Welsh, and T. Oomen, "Identification of additive continuous-time systems in open and closed loop," *Electrical Engineering and Systems Science*, vol. 2, 2024, doi: 10.48550/arXiv.2401.01263.

[38] M. Cheng, J. Zhou, W. Qian, B. Wang, C. Zhao, and P. Han, "Advanced electrical motors and control strategies for high-quality servo systems - a comprehensive review," *Chinese Journal of Electrical Engineering*, vol. 10, no. 1, pp. 63–85, Mar. 2024, doi: 10.23919/CJEE.2023.000048.

[39] R. Takarli *et al.*, "A comprehensive review on flywheel energy storage systems: survey on electrical machines, power electronics converters, and control systems," *IEEE Access*, vol. 11, pp. 81224–81255, 2023, doi: 10.1109/ACCESS.2023.3301148.

[40] K. Jankowska and M. Dybkowski, "Experimental analysis of the current sensor fault detection mechanism based on neural networks in the PMSM drive system," *Electronics*, vol. 12, no. 5, p. 1170, Feb. 2023, doi: 10.3390/electronics12051170.

BIOGRAPHIES OF AUTHORS

Vita Ayu Nathalia was born in Surabaya, Indonesia, in 2002. She was a student at the Electrical Engineering Department, Telkom University, Indonesia. She is currently looking for an opportunity for a post-graduate scholarship in the electrical engineering field with a concentration in control and automation engineering. She can be contacted at email: vitaayn23@gmail.com.

Dimas Adiputra was born in Jakarta, Indonesia, in 1993. He received a Ph.D. degree in medical instrumentation from Universiti Teknologi Malaysia, Malaysia, in 2020. He is currently an assistant professor at the Electrical Engineering Department, Telkom University Surabaya, Indonesia. His research interests in control engineering applications include healthcare devices and the internet of things, where the ultimate goal is healthcare services or facilities that transcend the distance for everyone. He can be contacted at email: dimasze@telkomuniversity.ac.id.

Rifki Dwi Putranto was born in Surakarta, Indonesia, in 1995. He received a Magister degree in Design and Power System from Institute Technology Sepuluh Nopember, Indonesia, in 2022. He is currently a Lecturer at the Electrical Engineering Department, Telkom University Surabaya, Indonesia. His research interests in power engineering, renewable energy, and electric vehicle. He can be contacted at email: rifkidwi@telkomuniversity.ac.id.